Chiral pharmaceutical drug adsorption to natural and synthetic particulates in water and their desorption in simulated gastric fluid.

PETRIE, B., MOURA, D.S., LAWTON, L.A. and SANGANYADO, E.

2023

Journal of Hazardous Materials Advances 9 (2023) 100241

Contents lists available at ScienceDirect

Journal of Hazardous Materials Advances

journal homepage: www.elsevier.com/locate/hazadv

Chiral pharmaceutical drug adsorption to natural and synthetic particulates in water and their desorption in simulated gastric fluid

Bruce Petrie[a,*], Diana S. Moura[a], Linda A. Lawton[a], Edmond Sanganyado[b]

[a] School of Pharmacy and Life Sciences, Robert Gordon University, Aberdeen AB10 7GJ, United Kingdom
[b] Department of Applied Sciences, Northumbria University, Newcastle Upon Tyne NE1 8ST, United Kingdom

ARTICLE INFO

Keywords:
Plastic
Biopolymer
Pharmaceutical
Emerging contaminant
Enantiomer
Sorption

ABSTRACT

Natural and synthetic particulates in aquatic environments can act as a vector for chiral pharmaceutical drugs. Understanding enantiomer enrichment in the particulate phase of water matrices is essential considering the enantiospecific effects that chiral drugs can have on exposed organisms. Therefore, the enantiospecific adsorption of the cationic drugs fluoxetine and propranolol to polyhydroxyalkanoate bioplastic, polyamide microplastic, and cellulose particulates was investigated in 0.01 M calcium chloride ($CaCl_2$) buffer and real environmental matrices. Fluoxetine enantiomers adsorbed to all particulate types under all conditions studied. Yet, propranolol only adsorbed to polyamide in 0.01 M $CaCl_2$ buffer at pH 11, and in samples prepared using real matrices (river water and wastewater). No enantioselectivity was observed in the adsorption of fluoxetine or propranolol, or their subsequent desorption in a simulated gastric environment. Findings showed the enantiomeric composition of the adsorbed drug will reflect that of the dissolved drug assuming no degradation takes place. However, further enantiospecific adsorption studies are now needed on a broader range of chiral drugs and particulate matter found in water. Importantly, drug adsorption was considerably greater in river water and wastewater compared to 0.01 M $CaCl_2$ buffer (2.1 to 5.3 times for fluoxetine). Most adsorption studies reported in the literature use 0.01 M $CaCl_2$ buffer to conform with international guidelines for assessing the adsorption behaviour of chemicals. Although such conditions enable direct comparison with similar studies, they can underestimate cationic drug adsorption to particulates in engineered and natural environments. This needs consideration in future studies on drug adsorption to microplastics and other particulate matter in laboratory studies.

1. Introduction

There are concerns that particulate matter present in water, such as microplastics, can act as a vector of other pollutants. This includes pharmaceutical drugs which have known health effects on aquatic organisms (Fogliano et al., 2022; Medkova et al., 2022). Research has found that cationic drugs more hydrophobic in nature have the greatest propensity to *(i)* adsorb to synthetic microplastics in water, and *(ii)* desorb from the microplastic surface under a low pH gastric environment (McDougall et al., 2022). Several of the more hydrophobic cationic drugs are chiral, including antidepressants and some beta-blockers. Chiral drugs exist as two or more enantiomers which differ in their three-dimensional structure. Differences in shape mean enantiomers of the same drug can interact differently in biological environments. To date, environmental research on enantioselective behaviour of chiral drugs has focussed on their occurrence, degradation, and toxicity (Bagnall et al., 2013; Baker and Kasprzyk-Hordern, 2013; Andrés-Costa et al., 2017). Only a few studies have investigated the adsorption of chiral drugs at the enantiomeric level (Sanganyado et al., 2016; Chen et al., 2022). It is essential to improve the understanding of enantiospecific adsorption to suspended particulate matter to better predict the fate and effects of chiral drugs in the environment.

There is a variety of natural (e.g., cellulose) and synthetic particulate matter (e.g., microplastics) present in the aquatic environment. Nature particulates such as cellulose have several chiral centres in each repeating monomer which could result in different interactions with drug enantiomers. Indeed, cellulose based liquid chromatography stationary phases (derivatised with achiral reagents) are commonly applied to separate drug enantiomers for enantioselective analysis (Petrie et al., 2019). However, no previous study has investigated the enantiospecific adsorption of chiral drugs to cellulose in water. Sanganyado et al. (2016) investigated the enantiospecific adsorption of various beta-blockers to wastewater sludge (containing an expected mixture of natural and synthetic particulates) using controlled batch

* Corresponding author.
E-mail address: b.r.petrie@rgu.ac.uk (B. Petrie).

https://doi.org/10.1016/j.hazadv.2023.100241
Received 17 November 2022; Received in revised form 9 January 2023; Accepted 13 January 2023

laboratory experiments. Several drugs including *R/S(±)*-acebutolol and *R/S(±)*-metoprolol showed enantioselective adsorption with up to two-fold difference in enantiomer adsorption of the same drug.

Petroleum based microplastics in their manufactured form are not chiral in nature and therefore not expected to result in enantioselective drug adsorption. However, Elmer-Dixon et al. (2022) found that as polyethylene plastic aged it formed chiral nanostructures on its surface which could result in enantioselective adsorption. Chen et al. (2022) noted a small (3–5%) but significant difference in the adsorption of *R/S(±)*-ofloxacin and levofloxacin (*S(-)*-ofloxacin) to polyethylene microplastics. Unfortunately, enantioselective analysis was not performed to demonstrate differences in enantiomer adsorption in those experiments performed on the racemic drug. Numerous studies report non-linear adsorption isotherms for drugs and microplastics (Li et al., 2022; Sun et al., 2022; Wagstaff and Petrie, 2022), indicating a concentration dependant adsorption process. This could result in those drugs present in non-racemic composition in water being subject to enantioselective adsorption (causing differences between the drug enantiomeric composition in water and that adsorbed to particulate matter).

Concerns on the effects and persistence of plastics in the environment has led to the design and production of biodegradable plastic alternatives or bioplastics. Bioplastics such as polylactic acid and polyhydroxybutyrate/polyhydroxyvalerate co-polymers are derived from biological substances rather than petroleum. Resultantly, they have chiral structures which could see different interactions with drug enantiomers. Drug adsorption to bioplastic particulates has been established (Sun et al., 2022). However, no study has investigated drug adsorption at the enantiomeric level to bioplastic particulates.

A further consideration for drug enantiomer adsorption is their interaction with other chiral dissolved organic species in the water matrix. For example, humic acid is found in natural waters at comparatively greater concentrations than drugs. Studies found humic acid can influence drug adsorption to microplastics (Zhang et al., 2018). Humic acid can retain drugs in the aqueous phase if itself does not adsorb to particulate matter. Otherwise, humic acid that adsorbs to the particulate surface can act as a bridge for drug adsorption (Zhang et al., 2018). Humic acid has been found to adsorb to the more polar microplastics (e.g., polyamide) (Zhang and Bai, 2002), whereas it has little interaction with polyethylene (Wu et al., 2016). Therefore, it is important to undertake enantioselective adsorption studies in the presence of humic acid.

Suspended particulate matter can be ingested by cold- and warm-blooded aquatic organisms. Microplastics have been found in the gastrointestinal tract of birds, mammals, fish, and macroinvertebrate (Hoang and Mitten, 2022; Parker et al., 2022; Philipp et al., 2022). Numerous studies report considerable desorption of drugs (≥50% of the adsorbed concentration) from microplastics in a simulated low pH gastric environment (Lin et al., 2020; McDougall et al., 2022; Wagstaff et al., 2022). The role of enzymes (e.g., pepsin) in the desorption process may also result in enantioselectivity, different to that observed during metabolism. Liu et al. (2020) reported pepsin can enhance drug desorption by increasing drug solubility in solution as well as competing for adsorption sites on microplastics surfaces. Again, no data exists on the enantioselectivity of drugs during the desorption process.

The aim of this study was to address some of the knowledge gaps on the enantioselective adsorption and desorption of chiral drugs to and from suspended particulate in water. Enantiospecific adsorption to different particulates including polyhydroxybutyrate/polyhydroxyvalerate 1% bioplastic, polyamide, and cellulose, and their subsequent desorption in gastric fluids was investigated. Laboratory studies were utilised to enable close control of test conditions and to study particulates in isolation of others. The beta-blocker propranolol and the antidepressant fluoxetine were investigated due to their propensity to adsorb to particulate matter in water, and their ubiquity in the environment (Proctor et al., 2021).

2. Materials and methods

2.1. Materials

Reference standards of *R/S(±)*-propranolol hydrochloride, *S(-)*-propranolol hydrochloride, *R(+)*-propranolol hydrochloride, *R/S(±)*-fluoxetine hydrochloride, *S(+)*-fluoxetine hydrochloride and *R(-)*-fluoxetine hydrochloride were purchased from Sigma Aldrich (Gillingham, UK). High-performance liquid chromatography (HPLC) grade methanol and ammonium acetate, glacial acetic acid, calcium chloride ($CaCl_2$), GF/F glass fibre filter papers, 4 mm polyvinylidene fluoride (PVDF) 0.45 μm syringe filters, hydrochloric acid (HCl) and sodium hydroxide (NaOH) were obtained from Fisher Scientific (Loughborough, UK). Pepsin A (≥500 U mg^{-1}), sodium chloride (NaCl), humic acid and sodium azide (NaN_3) were purchased from Sigma Aldrich. Ultrapure water was 18.2 MΩ cm^{-1} quality. Bioplastic (polyhydroxybutyrate/polyhydroxyvalerate 1%) and polyamide (Nylon 12) were purchased from Goodfellow Cambridge Limited (Huntingdon, UK). Cellulose (microcrystalline) was obtained from Sigma Aldrich (see Table 1). Municipal wastewater (5 L) was collected from a septic tank and river water (5 L) from the River Don in North-East Scotland during October 2021 and frozen at −20 °C. Wastewater and river water did not contain detectable levels of propranolol and fluoxetine.

2.2. Microplastics characterisation

Attenuated Total Reflectance-Fourier Transform Infrared (ATR-FTIR) Spectroscopy analysis was used to confirm the material received from the supplier. The ATR-FTIR scanning wavenumber was set from 400 to 4000 cm^{-1}. The spectra were produced using 32 scans per sample at resolution of 4 cm^{-1} (Figure S1). The particle size distribution was evaluated using the Mastersizer 3000 Laser Diffraction Particle Size analyzer (Malvern Panalytical, UK). The zeta potential measurement was carried out in 0.01 M $CaCl_2$ buffer under different pH values (3, 5, 7, 9, and 11) using a Malvern Zetasizer (Nano ZS, UK). Scanning Electron Microscopy (SEM, EVO LS10, Carl Zeiss, UK) imaging was performed to evaluate the surface morphology of the particulates.

2.3. Adsorption experiments

Adsorption experiments were conducted in 0.01 M $CaCl_2$ in ultrapure water adjusted to pH 7.5. In 50 mL conical flasks 20 mL of 2500 mg L^{-1} bioplastic, polyamide or cellulose were prepared. These were kept in the dark and mixed at 220 rpm using a MaxQ 4000 orbital shaker (Thermo Scientific, Loughborough, UK) maintained at 20 °C. This ensured all particle types were fully mixed and evenly distributed in the water. Samples were mixed for one hour prior to spiking with drugs. Uptake kinetics and equilibrium time were established at a spiked racemic drug concentration of 1 mg L^{-1} (i.e., 0.5 mg L^{-1} of the individual enantiomers). This gave drug to particulate ratios similar to previous studies (Wu et al., 2016; Razanajatovo et al., 2018). Samples were collected following 0.5, 1, 2, 4, 6, 24, 48, 72 and 96 h mixing (Wagstaff and Petrie, 2022). The uptake kinetics were fitted using the pseudo-second order model:

$$q_t = \frac{q_e^2 kt}{1 + q_e kt} \quad (1)$$

Where q_t (mg kg^{-1}) is the adsorbed fluoxetine concentrations at any time, q_e (mg kg^{-1}) is the adsorbed enantiomer concentration under equilibrium, t (hours) is the mixing time and k (kg mg^{-1} h^{-1}) is the equilibrium rate constant.

Racemic drugs concentrations of 0.5, 1.0, 1.5, 2.0 and 2.5 mg L^{-1} were used to establish adsorption isotherms Wagstaff and Petrie, 2022). The Freundlich ((2) and Langmuir (3) isotherms were used to model the data:

$$q_e = K_F C_e^{1/n} \quad (2)$$

Table 1
Properties of the bioplastic, polyamide, and cellulose particulates.

Particulate material	Monomer	Size (μm)		Surface area (m^2 kg^{-1})	Zeta potential (mV)	SEM image[d]
		D_{50}	Range			
Bioplastic[a] (polyhydroxybutyrate/ polyhydroxyvalerate 1%)	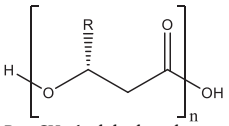 R = CH_3 (polyhydroxybutyrate) R = CH_2CH_3 (polyhydroxyvalerate)	13	1–310	790	−1.4 (pH 3) −19.0 (pH 5) −26.2 (pH 7) −27.1 (pH 9) −29.5 (pH 11)	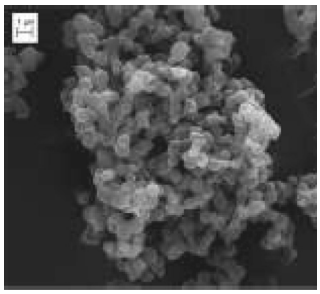
Polyamide (Nylon 12)[b]	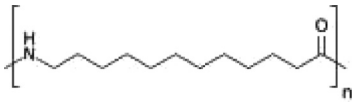	89	4–211	110	−4.6 (pH 3) −8.4 (pH 5) −14.8 (pH 7) −14.9 (pH 9) −16.8 (pH 11)	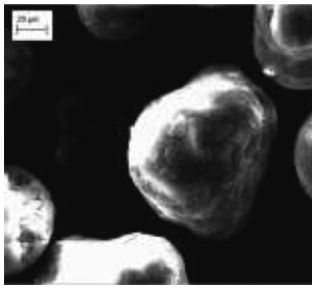
Cellulose (microcrystalline)[c]	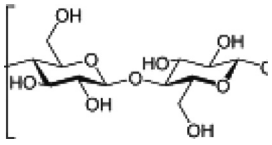	126	11–352	69	−2.3 (pH 3) −3.2 (pH 5) −5.5 (pH 7) −4.0 (pH 9) −5.5 (pH 11)	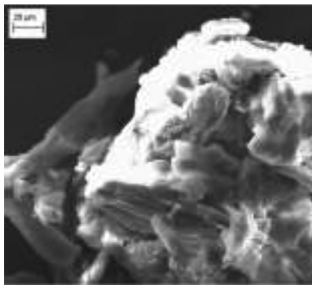

Note: the chemical composition of the different particulate material was confirmed by FTIR analysis (Figure S1).
[a] Manufacturer reported maximum size = 250 μm.
[b] Manufacturer reported maximum size = 250 μm; D_{50} = 90 μm.
[c] Manufacturer reported mean size = 90 μm.
[d] 10,000x magnification for bioplastic and 1,000x for polyamide and cellulose.

$$q_e = \frac{q_{max} K_L C_e}{1 + K_L C_e} \quad (3)$$

C_e (mg L^{-1}) is the remaining enantiomer concentration in water, K_F [(mg kg^{-1})(mg L^{-1})^n] and n are the Freundlich constants, K_L is the Langmuir constant (L mg^{-1}), and q_{max} (mg kg^{-1}) is the estimated maximum adsorption capacity. The data was modelled in Microsoft Excel using the Solver tool.

The influence of drug enantiomeric composition on adsorption was investigated at different drug enantiomeric fraction (EF) values of 0.1, 0.3, 0.5, 0.7 and 0.9 at 1 mg L^{-1} total drug concentration (sum of both enantiomers). The EF is used to describe the concentration of drug enantiomers relative to one another and calculated using:

$$EF = \frac{(+)}{(+) + (-)} \quad (4)$$

(+) is *R(+)*-propranolol or *S(+)*-fluoxetine, and *(-)* is *S(-)*-propranolol or *R(-)*-fluoxetine. The EF value can vary between 0 (when the concentration of *(+)* is zero) and 1 (when the concentration of *(−)* is zero) and an EF of 0.5 represents a racemic mixture of enantiomers.

The role of changing drug speciation and particulate surface charge on enantiomer adsorption was investigated by adjusting water pH (3, 5, 7, 9 and 11) using HCl or NaOH. The effect of dissolved organic matter on enantiomer adsorption was studied using humic acid concentrations at 0, 5, 10, 25 and 50 mg L^{-1}. Adsorption was also investigated in filtered wastewater and river water (instead of 0.01 M $CaCl_2$ buffer). For these experiments wastewater and river water was defrosted overnight, filtered through GF/F filters, and treated with 0.2 g L^{-1} sodium azide to limit any microbial activity. All samples were collected following 72 h of mixing. Water samples were filtered through 0.45 μm PVDF filters ready for enantioselective high-performance liquid chromatography-tandem mass spectrometry (HPLC-MS/MS) analysis. Equivalent experiments without particulates (control) to evaluate any pharmaceutical losses to glassware were utilised for all experiments, and to determine the adsorbed drug concentrations. All experiments were performed in triplicate.

2.4. Desorption experiments

Initially, adsorption experiments were conducted in 0.01 M $CaCl_2$ buffer (pH 7.5) at racemic drug concentrations of 2.5 mg L^{-1} as described in Section 2.2. Following 72 h mixing the particulates were collected and transferred into 20 mL gastric fluid (particulate concentra-

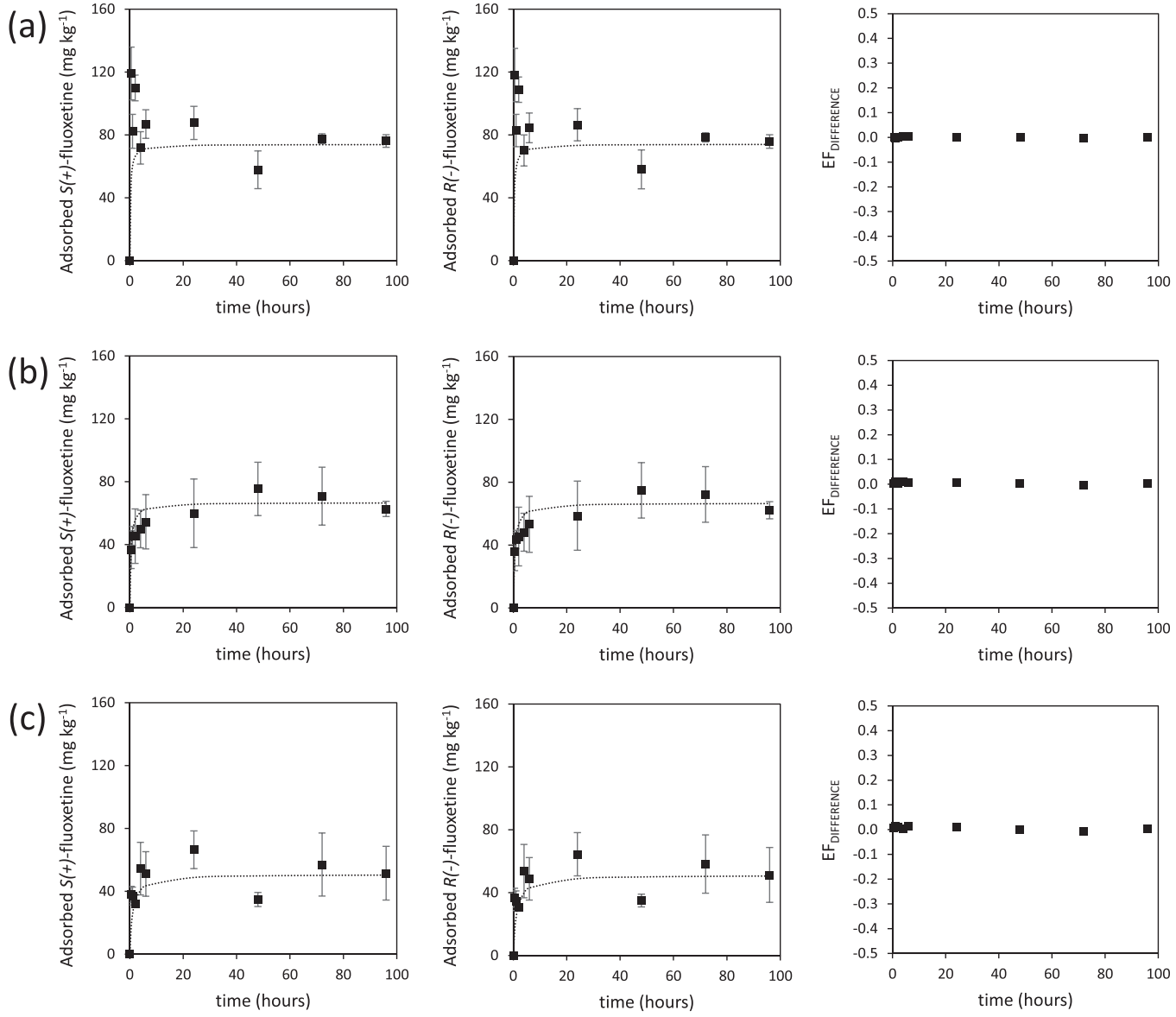

Fig. 1. Adsorption of *S(+)*-fluoxetine and *R(-)*-fluoxetine to bioplastic (a), polyamide (b) and cellulose (c) particulates in 0.01 M $CaCl_2$ buffer at pH 7.5 over 96 h, and the difference in enantiomeric fraction of the adsorbed drug compared to the enantiomeric fraction of the drug in water without particulates added ($EF_{DIFFERENCE}$). The dashed line represents the data fitted to the pseudo-second order model.

tion = 2500 mg L^{-1}). Simulated gastric fluids comprised 3.2 g L^{-1} pepsin A in 100 mM NaCl at pH 2 using HCl (Liu et al., 2020). Desorption studies were undertaken at 20 °C and 37 °C to mimic cold- and warm-blooded organism temperatures. Samples were mixed at 220 rpm using a MaxQ 4000 orbital shaker and collected at 15, 30, 60, and 120 min to encompass a typical gastric digestion time (Wang et al., 2011). Experiments were conducted on bioplastic, polyamide and cellulose and performed in triplicate. Experiments were also conducted without particulates at a 1 mg L^{-1} racemic drug concentration to determine any drug loses in the gastric fluid over the 120-minute study period.

2.5. Analytical methods

Enantiomer separation was performed using a Chirobiotic V2® HPLC column (250 × 2.1 mm; 5 μm) maintained at 11 °C. The mobile phase was methanol containing 1 mM ammonium acetate and 0.01% acetic acid operated under isocratic conditions with a flow rate of 0.35 mL min^{-1}. The injection volume was 4 μL and run time 19 minutes. An Agilent 1200 Infinity Series HPLC coupled to a 6420 triple quadrupole MS/MS (Cheshire, UK) was used for analysis. Positive electrospray ionisation (ESI) with a capillary voltage of 4000 V was used. Nitrogen was the nebulising, desolvation and collision gas. The desolvation temperature was 350 °C with a gas flow of 12 L min^{-1}. The nebulising pressure was 50 psi. Multiple reaction monitoring transitions for propranolol and fluoxetine is found in Table S1. Matrix matched calibrations (0.01 M $CaCl_2$ buffer, wastewater, river water or simulated gastric fluids) were used to account for any matrix specific signal suppression. The calibrations ranged from 0.01 to 3 mg L^{-1} of the racemic drug. An example chromatogram is shown (Figure S2).

3. Results and discussion

3.1. Adsorption of chiral drugs to particulate matter in water

Initially, the adsorption of *R/S(±)*-propranolol and *R/S(±)*-fluoxetine was investigated to polyhydroxybu-

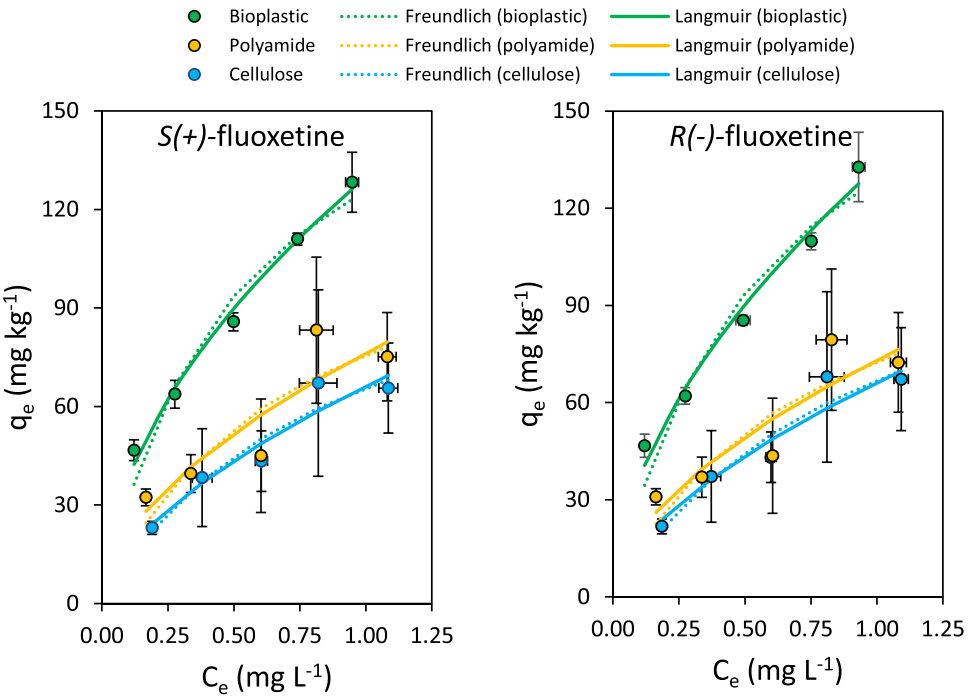

Fig. 2. Freundlich (broken line) and Langmuir isotherms (unbroken line) of *S(+)*-fluoxetine and *R(-)*-fluoxetine adsorption to bioplastic (green), polyamide (yellow) and cellulose (blue) particulates in 0.01 M $CaCl_2$ buffer at pH 7.5. Circles show the experimental data.

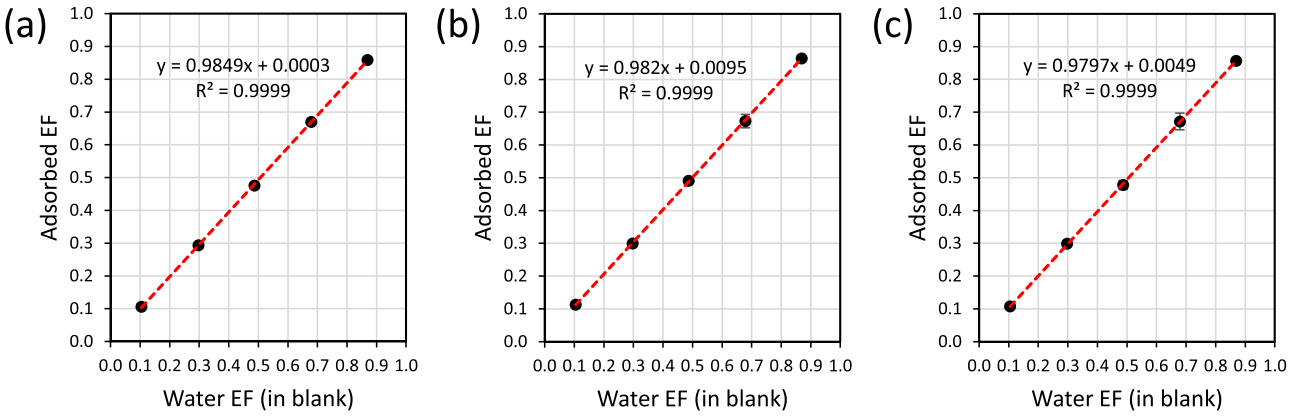

Fig. 3. Influence of fluoxetine enantiomeric fraction in 0.01 M $CaCl_2$ buffer at pH 7.5 (x-axis) on the enantiomeric fraction of fluoxetine adsorbed to bioplastic (a), polyamide (b) and cellulose (c) particulates (y-axis).

tyrate/polyhydroxyvalerate 1% bioplastic, polyamide and cellulose during 96 h mixing. Adsorption of fluoxetine enantiomers fitted the pseudo-second order kinetic model with coefficient of determination (r^2) values ≥0.946 suggesting that 94.6% of the variability in the data was described by the regression line (Table S2). Both the experimental and calculate q_e values compare well (Fig. 1; Table S2). Fluoxetine enantiomer adsorption followed the order; bioplastic (74 mg kg^{-1}) > polyamide (67 mg kg^{-1}) > cellulose (51 mg kg^{-1}) (Fig. 1; Table S2). Concha-Graña et al. (2022) found the adsorption of pesticides and personal care products was higher to polyhydroxybutyrate than polyamide. Bioplastics typically contain nanoscale pores which other pollutants can enter and become trapped (Ribba et al., 2022). However, it should be noted that the adsorption in our study increased with increasing surface area (and increasing negative surface charge) of the three particulate types (Table 1). Therefore, direct comparisons between particulate type in this study should be made with caution due to differences in their size and surface charge (Table 1).

Since adsorption proceeded rapidly (Fig. 1), subsequent experiments used 72 h mixing, aligning with previous studies investigating the drug adsorption to microplastics in 0.01 M $CaCl_2$ buffer (Razanajatovo et al., 2018; Elizalde-Velázquez et al., 2020). Interestingly, little difference in *S(+)*-fluoxetine and *R(-)*-fluoxetine adsorption was observed. No notable differences in fluoxetine EF values in control experiments and that adsorbed to the particulate material were observed (Fig. 1). Previous research indicates that the cationic speciation of fluoxetine coupled with its hydrophobicity are important for its adsorption (McDougall et al., 2022).

The adsorption of propranolol enantiomers was <5% and no measurable concentration difference was found in water between the control (no particulates) and test experiments (particulates removed by filtration following mixing). The less hydrophobic nature of propranolol compared to fluoxetine, as shown by its lower pH dependant octanol-water partition coefficient at pH 7.5 (log D_{OW} 1.55 compared to 1.75 – Figure S3), is likely to contribute to its lack of adsorption. However, previous research in environmental waters has found higher adsorption of propranolol to microplastics than observed in this study (McDougall et al., 2022; Wagstaff et al., 2022). Puckowski et al. (2021) showed that the sorption of pharmaceuticals, including propranolol, on polyethene,

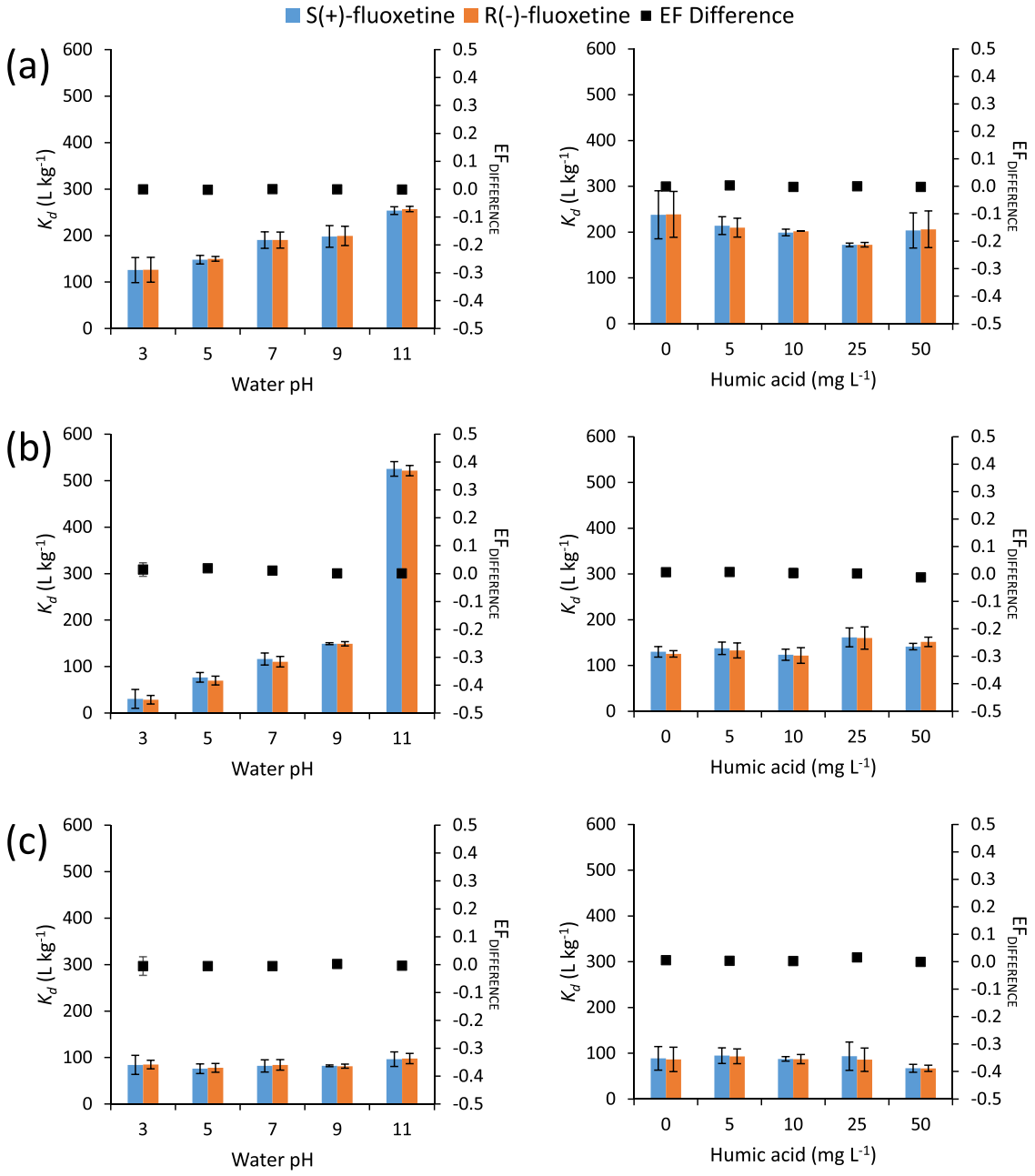

Fig. 4. Effect of water pH (left) and humic acid concentration (right) on adsorption of *S(+)*-fluoxetine and *R(-)*-fluoxetine to bioplastic (a), polyamide (b) and cellulose (c) particulates in 0.01 M $CaCl_2$ buffer (primary y-axis), and the difference in enantiomeric fraction of the adsorbed drug compared to the enantiomeric fraction of the drug in water without particulates added (secondary y-axis). Water containing different humic acid concentrations was kept constant at pH 7.5. K_d (L kg^{-1}) is the distribution coefficient between the particulate and water phases.

polypropylene, and polyvinyl chloride was negatively influenced by the ionic strength of the medium. Propranolol occurs predominantly in its cationic form at pH values below 9.52 (as does fluoxetine). It is possible that the low sorption of propranolol is due to chaotropic effect, whereby the $CaCl_2$ of the buffer acts as a chaotropic agent that disrupts hydrogen bonds between the polar functional groups of the particulates and propranolol. Propranolol has a hydroxyl functional group within its structure whereas fluoxetine does not (Figure S4). Chaotropic effect has been reported in lignocellulosic biomass (Zongo et al., 2019), chiral stationary phases (Flieger, 2009) and biofibers (Mittal et al., 2019). Therefore, hydrogen bonding (involving the hydroxyl functional group) may be the dominant adsorption interaction between propranolol and particulates in water. Whereas fluoxetine has a trifluoromethyl functional group within its structure leading to hydrophobic interactions (Figure S4).

Adsorption was assessed at individual enantiomer concentrations in water ranging from 0.25 to 1.25 mg L^{-1}. No adsorption of propranolol was noted at any of the studied concentrations. The adsorption data for fluoxetine enantiomers were fitted to the Langmuir and Freundlich isotherms with r^2 values in the range 0.766–0.980 (Fig. 2; Table S2). They had similar or greater r^2 values when fitted to the Freundlich isotherm compared to the Langmuir isotherm (Table S2). Fitting to the Freundlich isotherm indicates multilayer adsorption to the particulate surface and has been commonly used to model the adsorption of drugs to particulate matter (Zhang et al., 2018; Liu et al., 2019). There was no clear difference between the adsorption of individual enantiomers at

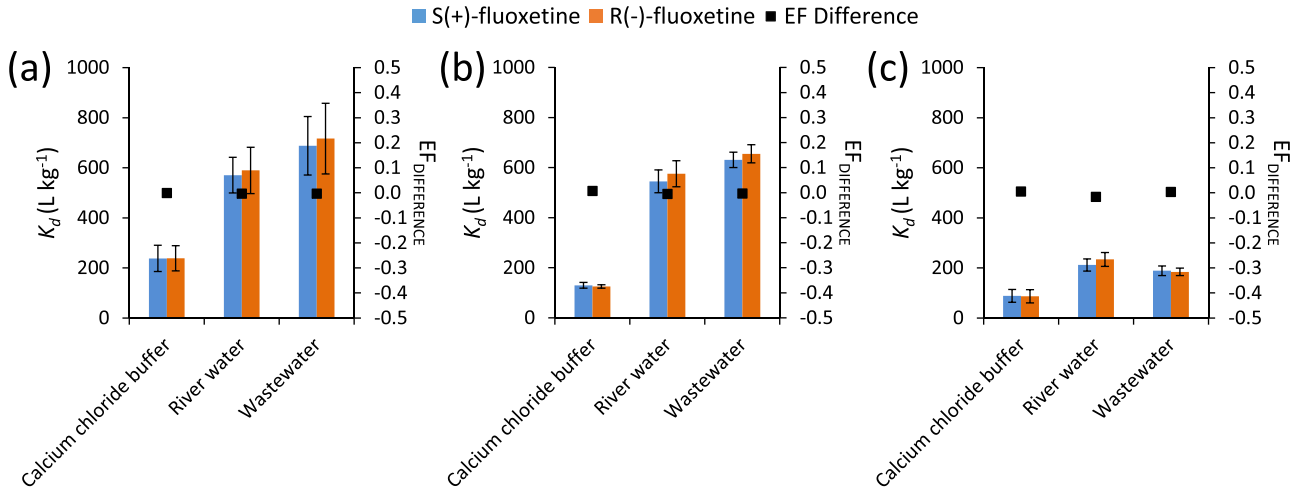

Fig. 5. Adsorption of *S(+)*-fluoxetine and *R(-)*-fluoxetine to bioplastic (a), polyamide (b) and cellulose (c) particulates in 0.01 M $CaCl_2$ buffer, river water and wastewater (primary y-axis), and the difference in enantiomeric fraction of the adsorbed drug compared to the enantiomeric fraction of the drug in water without particulates added (secondary y-axis). K_d (L kg^{-1}) is the distribution coefficient between the particulate and water phases.

each of the concentrations studied. However, the non-linear adsorption (greater adsorption at lower concentrations – see Fig. 2) suggests enantioselectivity in adsorption may be observed where the drug is already in non-racemic composition.

3.2. Enantiomeric fraction variation

The influence of drug EF on enantiomer adsorption was assessed at EF values of 0.1, 0.3, 0.5 (racemic), 0.7 and 0.9 (sum of both enantiomers = 1 mg L^{-1}). There was a close agreement between the measured EF in the blank (water with no particulates added) and the EF of adsorbed fluoxetine for all experiments (Fig. 3). This is despite an EF of 0.1 and 0.9 having a nine-fold difference in enantiomer concentration. The data used to model the isotherms had a five-fold difference between the minimum and maximum enantiomer concentrations. However, the isotherm data is generated from different total drug concentrations. It is postulated that as the drug concentration in water increases it begins to saturate the number of available preferential adsorption sites resulting in a reduced percentage of adsorbed drug. As the total drug concentration was constant where the EF was varied (1 mg L^{-1}), the same proportion of total drug was adsorbed and no enantiospecific adsorption occurred. Therefore, it can be expected that the EF adsorbed to particulate matter in aquatic environments will reflect the EF of the aqueous phase assuming no degradation takes place. Evans et al. (2015) reported a fluoxetine EF value of 0.7 in influent wastewater, effluent wastewater, and digested sludge.

3.3. Water pH

Mobile phase pH is an important optimisation parameter when manipulating enantiomer interactions with chiral stationary phases in HPLC analysis (Sanganyado et al., 2017). Therefore, it was anticipated that water pH may influence enantiomer specific adsorption to those chiral particulates studied (bioplastic and cellulose). Enantiomer adsorption was studied at pH values of 3, 5, 7, 9 and 11 to assess the influence of changing drug speciation and particulate surface charge on enantiomer adsorption. However, no enantioselectivity in adsorption was observed across the three particulate types at any of the pH values investigated (Fig. 4). Water pH did influence total fluoxetine adsorption. Adsorption to polyamide particulates increased from pH 3 to pH 9. Under these pH conditions the fluoxetine enantiomers are present in cationic form (Figure S3). The greater adsorption as pH increased was attributed to an increasing negative surface charge of the polyamide which encourages electrostatic interaction (Table 1).

Considerably greater fluoxetine adsorption to polyamide was observed at pH 11 than any other pH (Fig. 4). This was due to the drug being in non-ionic form at this water pH (Figure S3), resulting in the drug having greater affinity to the hydrophobic polyamide surface. This data showed a similar trend to fluoxetine adsorption to the same polyamide particulates in wastewater at different pH values (Wagstaff et al., 2022). Fluoxetine adsorption to the bioplastic increased with increased surface charge (Fig. 4; Table 1). However, enhanced adsorption at pH 11 was not observed due to the bioplastic not being as hydrophobic as polyamide. The difference in hydrophobicity was clear when conducting the experiments as the polyamide tended to aggregate together or 'stick' to glassware surfaces whereas the bioplastic (and cellulose) was uniformly mixed in the 0.01 M $CaCl_2$ buffer. Water pH had little effect on cellulose surface charge and fluoxetine adsorption.

The only pH conditions that resulted in measurable adsorption of propranolol enantiomers was to polyamide particulates at pH 11. The particulate-water distribution coefficients were 65±6 L kg^{-1} and 71±2 L kg^{-1} for *S(-)*-propranolol and *R(+)*-propranolol, respectively. Under these pH conditions propranolol is in non-ionic form (Figure S3), enabling hydrophobic interaction with the non-polar polyamide surface (like the adsorption behaviour observed for fluoxetine).

3.4. Humic acid and real matrices

Humic acid concentrations up to 50 mg L^{-1} had little influence on the enantioselectivity of fluoxetine or its adsorption (Fig. 4). However, environmental matrices such as river water and wastewater comprise a diverse range of dissolved organic species that can influence drug-particulate interactions. Interestingly, although no enantioselectivity in fluoxetine adsorption occurred, both river water and wastewater resulted in enhanced enantiomer adsorption to all particulates studied (Fig. 5). Enantiomer adsorption was 2.1 to 5.3 times in river water or wastewater compared to 0.01 M $CaCl_2$ buffer. The greatest difference in adsorption was observed for polyamide particulates. Measurable, albeit low adsorption was found for propranolol enantiomers in the samples prepared using environmental matrices (45–67 L kg^{-1} for bioplastic; 90–109 L kg^{-1} for polyamide; 52–63 L kg^{-1} for cellulose), however, no enantioselectivity was observed.

Enhanced adsorption of pharmaceuticals in real environmental matrices is significant as most adsorption studies are un-

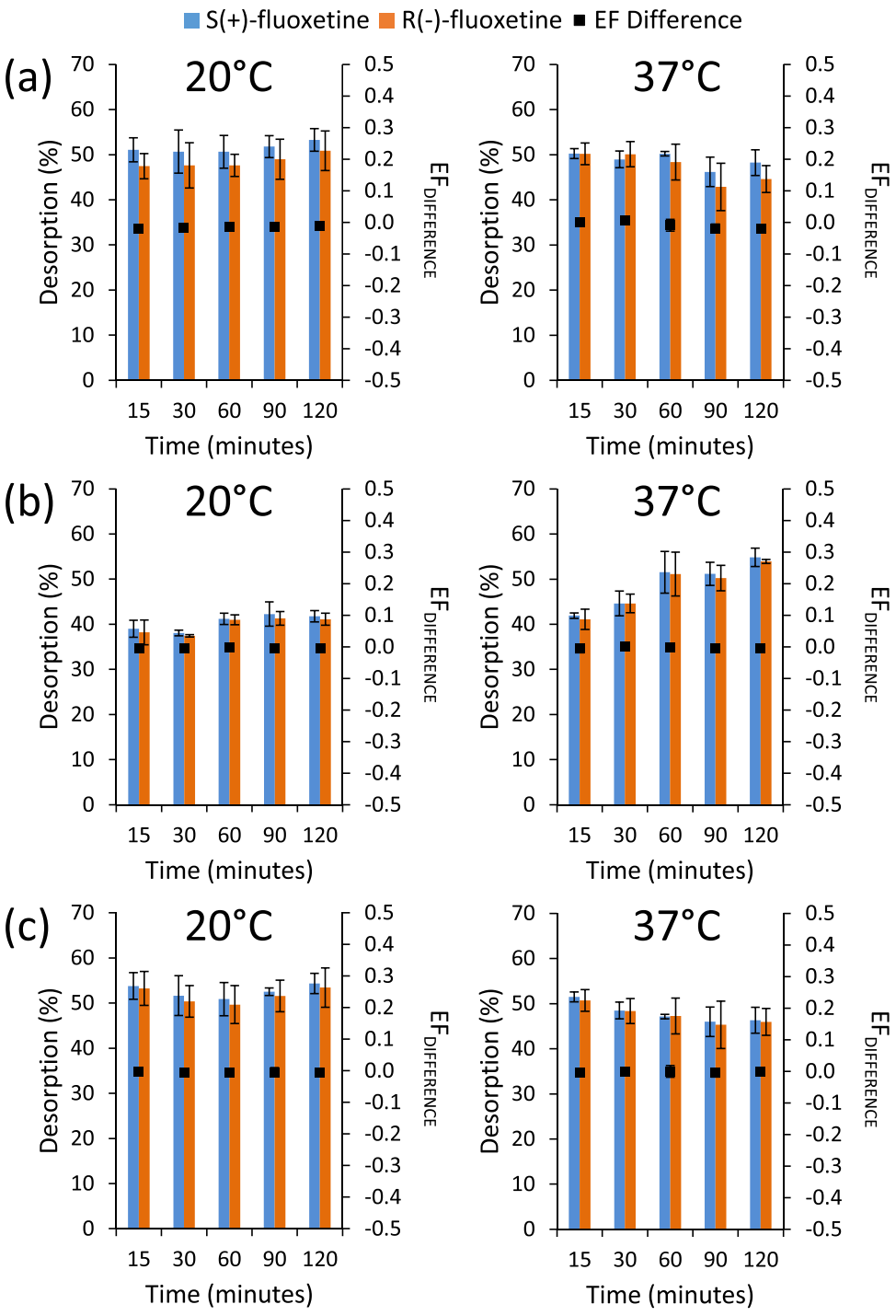

Fig. 6. Desorption of *S(+)*-fluoxetine and *R(-)*-fluoxetine from bioplastic (A), polyamide (B) and cellulose (C) particulates in simulated gastric fluids incubated at 20 °C and 37 °C (primary y-axis), and the difference in enantiomeric fraction of the desorbed drug in gastric fluid compared to the enantiomeric fraction of the adsorbed drug (secondary y-axis).

dertaken in controlled laboratory conditions using 0.01 $CaCl_2$ buffer (Razanajatovo et al., 2018; Elizalde-Velázquez et al., 2020; Puckowski et al., 2021). Tramadol, a cationic drug, was found to have significantly greater adsorption to soil from wastewater effluent compared to 0.01 M $CaCl_2$ buffer (Garduño-Jiménez et al., 2022). Reduced adsorption of fluoxetine observed in our study could be a result of Ca^{2+} ions competing for adsorption sorption sites and reducing the particulate surface charge, whereas the lack of propranolol adsorption is caused by chaotropic effect as previously discussed. Although adsorption studies using $CaCl_2$ buffer conform to the Organisation for Economic Cooperation and Development 106 Guideline (OECD, 2000), enabling direct comparison of studies across the literature, they can underestimate the adsorption of cationic pharmaceuticals to particulates in the environment.

3.5. Desorption

Fluoxetine enantiomers were found to be unchanged in simulated gastric fluids over 120 min exposure (Figure S5). Propranolol was not investigated due to its low adsorption to all studied particulates in 0.01 M $CaCl_2$, not enabling desorption to be investigated. Therefore, any changes observed during the desorption experiments were a result of the desorption process over transformation caused by pepsin. Fluoxetine enantiomer desorption reached ~50% from bioplastic and

cellulose particulates at both 20 °C and 37 °C (Fig. 6). There is limited data available on the desorption of drugs from bioplastics. However, Fan et al. (2021) also reported considerable desorption (>50%) of tetracycline and ciprofloxacin from virgin and aged bioplastics (polylactic acid) in simulated intestinal fluids. Little difference in desorption was observed over 120 min for bioplastic or cellulose particulates. Previous research has found desorption from microplastics to proceed rapidly in gastric fluid (Liu et al., 2020; Wagstaff and Petrie, 2022).

Fluoxetine desorption from polyamide was ~40% at 20 °C. However, desorption increased from 40% at 15 min incubation to 50% following 120 min incubation at 37 °C (Fig. 6). This can be important considering a typical gastric retention time is 120 min (Wang et al., 2011). Increased drug desorption from polyamide particulates at greater incubation temperatures was previously observed (Lin et al., 2020; Wagstaff et al., 2022). The difference in risk posed by adsorbed fluoxetine on polyamide particulates to cold- and warm-blooded organisms is expected to be greater at lower environmental temperatures. Importantly, no enantioselectivity in the desorption of fluoxetine was observed. Overall, there was little difference in desorption of fluoxetine enantiomers between the natural and synthetic particulates studied.

4. Conclusions and future research

The study revealed that fluoxetine enantiomers adsorbed to polyhydroxyalkanoate bioplastic, polyamide microplastic, and cellulose particulates in 0.01 M $CaCl_2$ buffer, but without any enantioselectivity. Subsequent desorption in gastric fluid was not enantioselective. Although enantioselectivity in adsorption was not observed in real matrices (wastewater and river water), there was enhanced enantiomer adsorption compared to 0.01 M $CaCl_2$ buffer. This is an important consideration for future studies that investigate the interaction of drugs with particulates in water. Despite a lack of enantioselectivity in adsorption observed for propranolol and fluoxetine in this study, there is a need to assess their adsorption to other particulate material found in water (including those pre-exposed to environmental conditions resulting in a weathered surface). Furthermore, a broader range of chiral drugs need investigated to better understand enantioselectivity in adsorption.

Funding information

Support by the Royal Society of Edinburgh is greatly appreciated.

Declaration of Competing Interest

The authors declare that they have no known competing financial interests or personal relationships that could have appeared to influence the work reported in this paper.

Data Availability

Data will be made available on request.

Acknowledgements

Support by the Royal Society of Edinburgh is greatly appreciated.

Supplementary materials

Supplementary material associated with this article can be found, in the online version, at doi:10.1016/j.hazadv.2023.100241.

References

Andrés-Costa, M.J., Proctor, K., Sabatini, M.T., Gee, A.P., Lewis, S.E., Pico, Y., 2017. Kasprzyk-Hordern, B. Enantioselective transformation of fluoxetine in water and its ecotoxicological relevance. Sci. Rep. 7 (1). doi:10.1038/s41598-017-15585-1, art. no. 15777.

Bagnall, J., Malia, L., Lubben, A., 2013. Kasprzyk-Hordern, B. Stereoselective biodegradation of amphetamine and methamphetamine in river microcosms. Water Res. 47 (15), 5708–5718. doi:10.1016/j.watres.2013.06.057.

Baker, D.R., Kasprzyk-Hordern, B., 2013. Spatial and temporal occurrence of pharmaceuticals and illicit drugs in the aqueous environment and during wastewater treatment: new developments. Sci. Total Environ. 454-455, 442–456. doi:10.1016/j.scitotenv.2013.03.043.

Chen, Y., Qian, Y., Shi, Y., Wang, X., Tan, X., An, D., 2022. Accumulation of chiral pharmaceuticals (ofloxacin or levofloxacin) onto polyethylene microplastics from aqueous solutions. Sci. Total Environ. 823. doi:10.1016/j.scitotenv.2022.153765, art. no. 153765.

Concha-Graña, E., Moscoso-Pérez, C.M., López-Mahía, P., Muniategui-Lorenzo, S., 2022. Adsorption of pesticides and personal care products on pristine and weathered microplastics in the marine environment. Comparison between bio-based and conventional plastics. Sci. Total Environ. 848. doi:10.1016/j.scitotenv.2022.157703, art. no. 157703.

Elizalde-Velázquez, A., Subbiah, S., Anderson, T.A., Green, M.J., Zhao, X., Cañas-Carrell, J.E., 2020. Sorption of three common nonsteroidal anti-inflammatory drugs (NSAIDs) to microplastics. Sci. Total Environ. 715. doi:10.1016/j.scitotenv.2020.136974, art. no. 136974.

Elmer-Dixon, M.M., Fawcett, L.P., Hinderliter, B.R., Maurer-Jones, M.A., 2022. Could superficial chiral nanostructures be the reason polyethylene yellows as it ages? ACS Appl. Polym. Mater. 4 (9), 6458–6465. doi:10.1021/acsapm.2c00877.

Evans, S.E., Davies, P., Lubben, A., Kasprzyk-Hordern, B., 2015. Determination of chiral pharmaceuticals and illicit drugs in wastewater and sludge using microwave assisted extraction, solid-phase extraction and chiral liquid chromatography coupled with tandem mass spectrometry. Anal. Chim. Acta 882, 112–126. doi:10.1016/j.aca.2015.03.039.

Fan, X., Zou, Y., Geng, N., Liu, J., Hou, J., Li, D., Yang, C., Li, Y., 2021. Investigation on the adsorption and desorption behaviors of antibiotics by degradable MPs with or without UV ageing process. J. Hazard. Mater. 401. doi:10.1016/j.jhazmat.2020.123363, art. no. 123363.

Flieger, J., 2009. Improvement of chiral discrimination of acidic enantiomers on teicoplanin stationary phase by the use of chaotropic effect. J. Liq. Chromatogr. Rel. Technol. 32 (7), 948–963. doi:10.1080/10826070902787401.

Fogliano, C., Motta, C.M., Venditti, P., Fasciolo, G., Napolitano, G., Avallone, B., Carotenuto, R., 2022. Environmental concentrations of a delorazepam-based drug impact on embryonic development of non-target Xenopus laevis. Aquat. Toxicol. 250. doi:10.1016/j.aquatox.2022.106244, art. no. 106244.

Garduño-Jiménez, A.-.L., Durán-Álvarez, J.C., Cortés-Lagunes, R.S., Barrett, D.A., Gomes, R.L., 2022. Translating wastewater reuse for irrigation from OECD Guidelines: tramadol sorption and desorption in soil-water matrices. Chemosphere 305. doi:10.1016/j.chemosphere.2022.135031, art. no. 135031.

Hoang, T., Mitten, S., 2022. Microplastic accumulation in the gastrointestinal tracts of nestling and adult migratory birds. Sci. Total Environ. 838. doi:10.1016/j.scitotenv.2022.155827, art. no. 155827.

Li, J., Huang, X., Hou, Z., Ding, T., 2022. Sorption of diclofenac by polystyrene microplastics: kinetics, isotherms and particle size effects. Chemosphere 290. doi:10.1016/j.chemosphere.2021.133311, art. no. 133311.

Lin, L., Tang, S., Wang, X.S., Sun, X., Han, Z., Chen, Y., 2020. Accumulation mechanism of tetracycline hydrochloride from aqueous solutions by nylon microplastics. Environ. Technol. Innov. 18. doi:10.1016/j.eti.2020.100750, art. no. 100750.

Liu, G., Zhu, Z., Yang, Y., Sun, Y., Yu, F., Ma, J., 2019. Sorption behavior and mechanism of hydrophilic organic chemicals to virgin and aged microplastics in freshwater and seawater. Environ. Pollut. 246, 26–33. doi:10.1016/j.envpol.2018.11.100.

Liu, P., Wu, X., Liu, H., Wang, H., Lu, K., Gao, S., 2020. Desorption of pharmaceuticals from pristine and aged polystyrene microplastics under simulated gastrointestinal conditions. J. Hazard. Mater. 392. doi:10.1016/j.jhazmat.2020.122346, art. no. 122346.

Medkova, D., Lakdawala, P., Hodkovicova, N., Blahova, J., Faldyna, M., Mares, J., Vaclavik, J., Doubkova, V., Hollerova, A., Svobodova, Z., 2022. Effects of different pharmaceutical residues on embryos of fish species native to Central Europe. Chemosphere 291. doi:10.1016/j.chemosphere.2021.132915, art. no. 132915.

McDougall, L., Thomson, L., Brand, S., Wagstaff, A., Lawton, L.A., Petrie, B., 2022. Adsorption of a diverse range of pharmaceuticals to polyethylene microplastics in wastewater and their desorption in environmental matrices. Sci. Total Environ. 808. doi:10.1016/j.scitotenv.2021.152071, art. no. 152071.

Mittal, N., Gordeyeva, K., Söderberg, L.D., Mittal, N., Benselfelt, T., Wågberg, L., Söderberg, L.D., Mittal, N., Benselfelt, T., Roth, S.V., Wågberg, L., Ansari, F., Roth, S.V., 2019. Ion-specific assembly of strong, tough, and stiff biofibers. Adv. Mater. 131 (51), 18735–18742. doi:10.1002/ANGE.201910603.

OECD, 2000. OECD guideline for the testing of chemicals Adsorption - Desorption Using a Batch Equilibrium Method. doi:10.1787/9789264069602.

Parker, B., Andreou, D., Pabortsava, K., Barrow, M., Green, I.D., Britton, J.R., 2022. Microplastic loads within riverine fishes and macroinvertebrates are not predictable from ecological or morphological characteristics. Sci. Total Environ. 839. doi:10.1016/j.scitotenv.2022.156321, art. no. 156321.

Petrie, B., Camacho Muñoz, M.D., Martín, J., 2019. Stereoselective LC–MS/MS methodologies for environmental analysis of chiral pesticides. Trends Analyt. Chem. 110, 249–258. doi:10.1016/j.trac.2018.11.010.

Philipp, C., Unger, B., Siebert, U., 2022. Occurrence of microplastics in harbour seals (Phoca vitulina) and Grey Seals (Halichoerus grypus) from German waters. Animals 12 (5). doi:10.3390/ani12050551, art. no. 551.

Proctor, K., Petrie, B., Lopardo, L., Muñoz, D.C., Rice, J., Barden, R., Arnot, T., Kasprzyk-Hordern, B., 2021. Micropollutant fluxes in urban environment – A catchment

perspective. J. Hazard. Mater. 401. doi:10.1016/j.jhazmat.2020.123745, art. no. 123745.

Puckowski, A., Cwięk, W., Mioduszewska, K., Stepnowski, P., Białk-Bielińska, A., 2021. Sorption of pharmaceuticals on the surface of microplastics. Chemosphere 263. doi:10.1016/j.chemosphere.2020.127976, art. no. 127976.

Razanajatovo, R.M., Ding, J., Zhang, S., Jiang, H., Zou, H., 2018. Sorption and desorption of selected pharmaceuticals by polyethylene microplastics. Mar. Pollut. Bull. 136, 516–523. doi:10.1016/j.marpolbul.2018.09.048.

Ribba, L., Lopretti, M., Montes De Oca-Vásquez, G., Batista, D., Goyanes, S., Vega-Baudrit, J.R., 2022. Biodegradable plastics in aquatic ecosystems: latest findings, research gaps, and recommendations. Environ. Res. Lett. 17 (3). doi:10.1088/1748-9326/ac548d, art. no. 033003.

Sanganyado, E., Fu, Q., Gan, J., 2016. Enantiomeric selectivity in adsorption of chiral β-blockers on sludge. Environ. Pollut. 214, 787–794. doi:10.1016/j.envpol.2016.04.091.

Sanganyado, E., Lu, Z., Fu, Q., Schlenk, D., Gan, J., 2017. Chiral pharmaceuticals: a review on their environmental occurrence and fate processes. Water Res. 124, 527–542. doi:10.1016/j.watres.2017.08.003.

Sun, M., Yang, Y., Huang, M., Fu, S., Hao, Y., Hu, S., Lai, D., Zhao, L., 2022. Adsorption behaviors and mechanisms of antibiotic norfloxacin on degradable and nondegradable microplastics. Sci. Total Environ. 807. doi:10.1016/j.scitotenv.2021.151042, art. no. 151042.

Wagstaff, A., Lawton, L.A., Petrie, B., 2022. Polyamide microplastics in wastewater as vectors of cationic pharmaceutical drugs. Chemosphere 288. doi:10.1016/j.chemosphere.2021.132578, art. no. 132578.

Wagstaff, A., Petrie, B., 2022. Enhanced desorption of fluoxetine from polyethylene terephthalate microplastics in gastric fluid and sea water. Environ. Chem. Lett. 20 (2), 975–982. doi:10.1007/s10311-022-01405-0.

Wang, Z., Zhao, J., Song, L., Mashayekhi, H., Chefetz, B., Xing, B., 2011. Adsorption and desorption of phenanthrene on carbon nanotubes in simulated gastrointestinal fluids. Environ. Sci. Technol. 45 (14), 6018–6024. doi:10.1021/es200790x.

Wu, C., Zhang, K., Huang, X., Liu, J., 2016. Sorption of pharmaceuticals and personal care products to polyethylene debris. Environ. Sci. Pollut. Res. Int. 23 (9), 8819–8826. doi:10.1007/s11356-016-6121-7.

Zhang, X., Bai, R., 2002. Adsorption behavior of humic acid onto polypyrrole-coated nylon 6,6 granules. J. Mater. Chem. 12 (9), 2733–2739. doi:10.1039/b201364a.

Zhang, H., Wang, J., Zhou, B., Zhou, Y., Dai, Z., Zhou, Q., Chriestie, P., Luo, Y., 2018. Enhanced adsorption of oxytetracycline to weathered microplastic polystyrene: kinetics, isotherms and influencing factors. Environ. Pollut. 243, 1550–1557. doi:10.1016/j.envpol.2018.09.122.

Zongo, L., Lange, H., Crestini, C., 2019. A study of the effect of kosmotropic and chaotropic ions on the release characteristics of lignin microcapsules under stimuli-responsive conditions. ACS Omega 4 (4), 6979–6993. doi:10.1021/acsomega.8b03510.

Supplementary information

Chiral pharmaceutical drug adsorption to natural and synthetic particulates in water and their desorption in simulated gastric fluid

Bruce Petrie[a]*; Diana Souza Moura[a]; Linda A. Lawton[a]; Edmond Sanganyado[b]

[a]School of Pharmacy and Life Sciences, Robert Gordon University, Aberdeen AB10 7GJ, UK

[b]Department of Applied Sciences, Northumbria University, Newcastle Upon Tyne NE1 8ST, UK

*Corresponding author email: b.r.petrie@rgu.ac.uk

The supplementary information contains four figures and two tables including FTIR spectra, enantioselective chromatograms, drug speciation at varying pH values, fluoxetine concentrations in gastric fluid incubations, MRM transitions as well as kinetics and isotherm data.

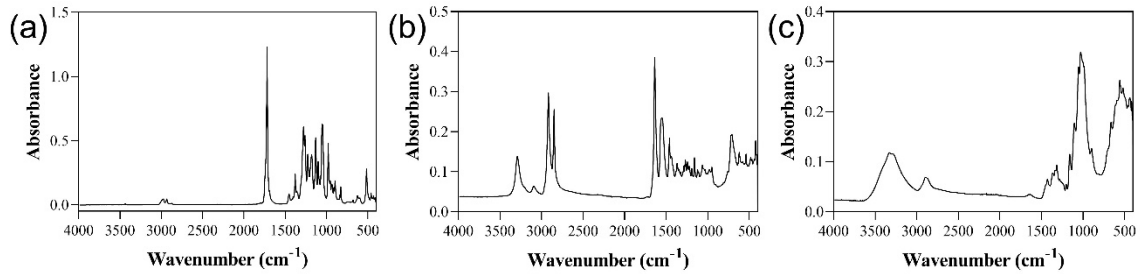

Figure S1. Attenuated Total Reflectance-Fourier Transform Infrared (ATR-FTIR) spectra of the bioplastic (A), polyamide (B) and cellulose (C) particulates

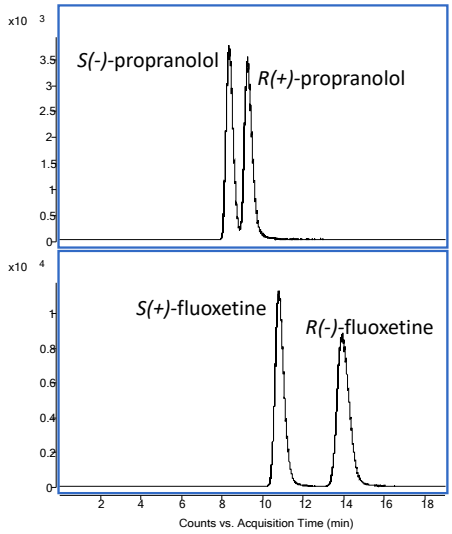

Figure S2. Enantioselective HPLC-MS/MS chromatograms of racemic propranolol and fluoxetine at 1 mg L^{-1} in 0.01 M $CaCl_2$ buffer

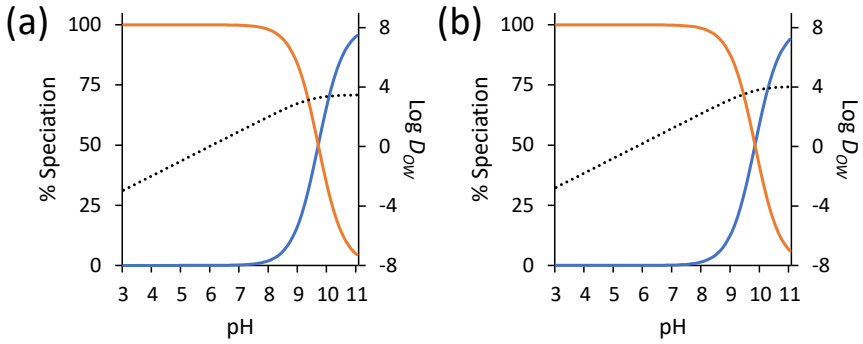

Figure S3. Speciation of propranolol (A) and fluoxetine (B) at different pH values. The pH dependant octanol-water partition coefficient (log D_{OW}) is presented on the secondary y-axis. Data obtained from ChemAxon (2021) and Pubchem (2021). The orange line represents the cationic species, the blue line is the neutral (non-ionised) species, and the broken black line is the log D_{OW}

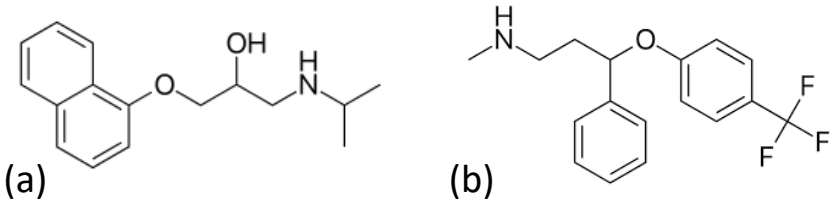

Figure S4. Structures of propranolol (a) and fluoxetine (b)

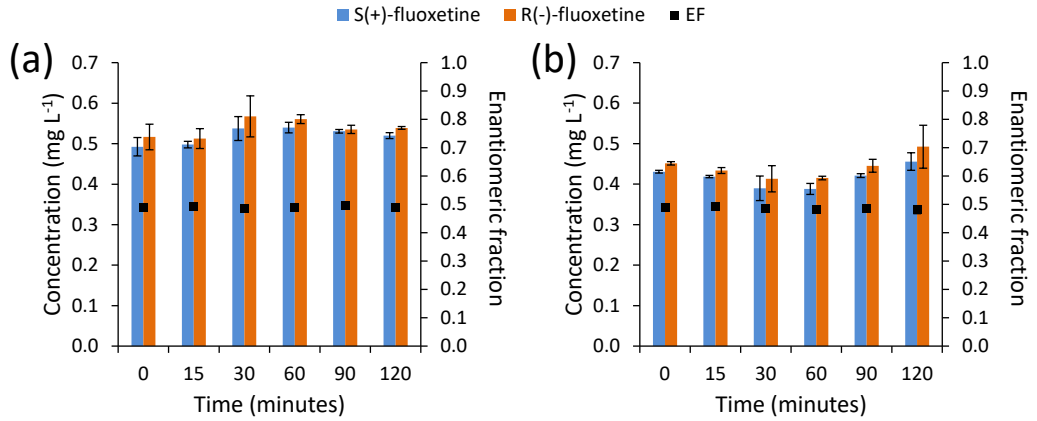

Figure S5. Fluoxetine concentration and enantiomeric fraction in gastric fluid at 20 °C and 37 °C over 120 minutes

Table S1. Multiple reaction monitoring parameters for propranolol and fluoxetine

Drug	Precursor (m/z)	Cone voltage (V)	Product 1 (m/z)	Collision energy (eV)	Product 2 (m/z)	Collision energy (eV)
R/S(±)-propranolol	259.9	110	115.9	10	182.9	10
R/S(±)-fluoxetine	309.8	90	44.0	2	147.7	10

Table S2. Kinetics and isotherm data for fluoxetine and bioplastic, polyamide, and cellulose particulates in 0.01 M $CaCl_2$ buffer

Model	Type	Parameter	Bioplastic		Polyamide		Cellulose	
			***S(+)*-fluoxetine**	***R(-)*-fluoxetine**	***S(+)*-fluoxetine**	***R(-)*-fluoxetine**	***S(+)*-fluoxetine**	***R(-)*-fluoxetine**
Kinetics	Pseudo-second order	q_e (mg kg^{-1})	74.0	74.1	66.6	66.7	50.8	51.1
		k (kg mg^{-1} h^{-1})	0.0586	0.0489	0.0374	0.0293	0.0196	0.0172
		r^2	0.979	0.980	0.991	0.988	0.946	0.946
Isotherm	Freundlich	K_F [(mg kg^{-1})(mg $L^{-1})^{1/n}$]	130	133	76.0	73.0	66.0	66.0
		n	1.89	1.79	1.80	1.77	1.65	1.65
		r^2	0.991	0.980	0.790	0.810	0.915	0.916
	Langmuir	q_{max} (mg kg^{-1})	190	205	130	128	123	135
		K_L (L mg^{-1})	1.95	1.69	1.40	1.32	1.15	0.987
		r^2	0.955	0.940	0.766	0.782	0.919	0.924

References

ChemAxon, 2021. Calculator Plugins were used for structure property prediction and calculation, Marvin 20.16.0. http://www.chemaxon.com Accessed 15/02/21.

Pubchem, Maryland, USA, 2021. National Institutes of Health. Accessed 05/01/21 https://pubchem.ncbi.nlm.nih.gov